PCCP

Accepted Manuscript

ROYAL SOCIETY OF CHEMISTRY

www.rsc.org/pccp

Journal Name

RSCPublishing

ARTICLE

Intramolecular charge transfer character in tetrathiafulvalene-annulated porphyrinoids: Effects of core modification and protonation†

Cite this: DOI: 10.1039/x0xx00000x

Received 00th January 2012,
Accepted 00th January 2012

DOI: 10.1039/x0xx00000x

www.rsc.org/

Ramababu Bolligarla,[a] Masatoshi Ishida,*[,b] Vijayendra S. Shetti,[c] Kazuhisa Yamasumi[b], Hiroyuki Furuta[b] and Chang-Hee Lee*[,a],

Synthesis, characterization, photophysical and electrochemical properties of novel tetrathiafulvalene (TTF)-annulated core-modified porphyrin (**1**) and its expanded rubyrin analogue (**2**) are described. The sulfur core modifications effected in **1** and **2** allow a feasible intramolecular charge transfer from the TTF fragments to central conjugated core as inferred from comparative spectroscopic and electrochemical measurements. DFT calculations also support the intramolecular charge transfer nature of **1** and **2** upon excitation. Further electronic perturbation of the TTF-annulated porphyrins was achieved by protonation, giving rise to drastic change in the optical feature with an extremely low energy band in the NIR region. The pronounced electron acceptor ability of the macrocyclic core of the dicationic species ($\mathbf{H_2}\mathbf{1}^{2+}$ and $\mathbf{H_2}\mathbf{2}^{2+}$) resulted in the thermally excited electron transfer occurring at room temperature as elucidated by EPR spectroscopy.

Introduction

Tetrathiafulvalene (TTF)-based molecular materials have received tremendous attentions over the years because of the excellent physical nature such as superconductivity, redox, magnetic and photophysical properties.[1] Extensive applications with electron donor-acceptor conjugates including nonlinear optical materials, photovoltaic solar cells, organic field-effect transistors and metal cation sensors have been thus developed.[2] A TTF molecule is indeed known to be involved in rich redox chemistry; TTFs can exist in any of three distinct stable redox states such as TTF^0, $TTF^{\bullet+}$ and TTF^{2+}. Over the past decade, the synthetic TTF derivatives hybridized with other π-electron rich acceptor molecules such as calixpyrroles[3] and porphyrins[4] would thus be expected to create intriguing systems with an essence of designed donor-acceptor (D-A) scaffolds.

The inherent charge transfer character present in a various TTF-annulated porphyrins (e.g., **3-6**) conjugated through their β-pyrrolic positions has been investigated to gain insight into the structure-property relationship by varying the number and position of TTF fragments on the conjugated core[4] as well as the size of π-network of the acceptor unit[5] (Chart 1). Such donor-acceptor annulated ensembles reported previously have been thought to allow stronger electronic coupling interactions between the donor and acceptor components due to the controlled structural natures; compact distances, parallel orientations and rigidified skeletons. For further fine tuning of the photo-induced charge transfer process, reduction potentials of acceptor (porphyrin) units seem to be critical variables.

The core-modifications of porphyrins and expanded porphyrins by replacing core NH with other hetero atoms (S, Se, Te and O) can alter their inherent structural and electronic properties, while the basic aromatic nature is preserved as similar to their parent pyrrolic congeners.[6] The overall photophysical (e.g., reasonably larger emission quantum yields and longer excited state dynamics) and electrochemical (e.g., facile reduction potentials) properties are expected to function as good acceptor units in these D-A ensembles. Furthermore, the sulfur core modified analogues has been shown the good photochemical stabilities as well as suitable HOMO and LUMO energy levels.[6]

In this study, hybrid macrocycles composing of photoactive core-modified porphyrinoids and electroactive TTFs fused at the pyrrole positions, namely TTF-annulated dithiaporphyrin (**1**) and tetrathiarubyrin (**2**) were synthesized and characterized as the first examples of donor-acceptor TTF-annulated, core modified porphyrins (Chart 1). The intramolecular charge transfer character from the TTF fragments to the porphyrin core was examined by comparable spectroscopic techniques and electrochemical measurements. The visualization of their electron flow upon an excitation was shown by DFT-based theoretical calculations. Furthermore, protonation, known as the ubiquitous phenomenon in the nitrogen-incorporated

porphyrinoids[7], drastically altered their electronic properties of the TTF-core modified porphyrins. Due to the enhanced electron acceptor ability of the macrocyclic core of the dicationic species ($\mathbf{H_21}^{2+}$ and $\mathbf{H_22}^{2+}$), an intermolecular thermal electron transfer occurred at room temperature along with emergence of lower energy NIR absorptions.

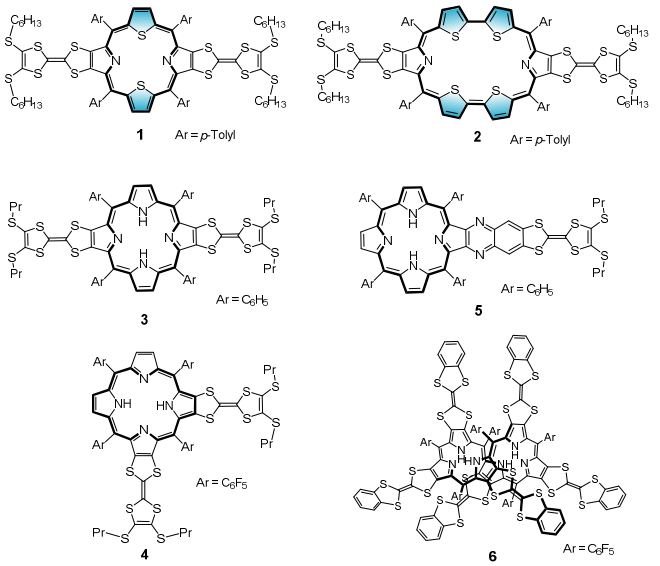

Chart 1. Chemical structures of TTF-annulated porphyrins and the higher derivative.

Experimental Section

Instruments. ^{1}H-NMR (300 MHz) and ^{13}C-NMR(100 MHz) spectra were recorded on a Bruker spectrometer. Chemical shifts (δ-scale, ppm) were referenced to the residual solvent peaks (δ of 5.32 for proton and 53.8 for carbon for dichloromethane). MALDI-TOF mass spectra were recorded on a Voyager-DE STR spectrometer using dithranol (1,8,9-trihydroxyantharacene) as a matrix. High-resolution mass spectra (HR-MS) were recorded on a JEOL JMS-700 FAB mass spectrometer with *m*-nitrobenzyl alcohol (NBA) as a matrix. HPLC analysis was performed on a JAI LC-9201 apparatus using preparative JAIGEL-SIL columns using CH_2Cl_2 as eluent. UV/vis/NIR absorption spectra were recorded on a Shimadzu UV-3150PC spectrometer. Emission spectra were recorded on a HORIBA SPEX Fluorolog-3 spectrometer. The electron paramagnetic resonance (EPR) measurement was carried out by a JOEL JES-FE1C X-band spectrometer. The light irradiation was performed by an Asahi spectra Xenon Light Source MAX300 (300W) with band path filters. Cyclic voltametric measurements were carried out on an ALS CHI 620B electrochemical analyzer using a conventional three-electrode cell for samples (1 mM) dissolved in dry dichloromethane containing 0.1 M nBu$_4$NPF$_6$ (TBA•PF$_6$) under an argon atmosphere. A glassy carbon working electrode, a platinum wire counter electrode, and an Ag/Ag$^+$ reference electrode were used in all the experiments. The potentials were calibrated using the ferrocenium/ferrocene couple.

Materials. All reagents and solvents were obtained from highest grade commercial sources and used without further purification unless otherwise noted. Analytical thin-layer chromatography (TLC) was performed on Merck silica gel 60 pre-coated aluminium sheets. Column chromatography was performed over basic alumina, Brockmann Grade I. 4,5-Bis(hexylthio)-1,3-dithiole-2-thione,[8] 5-tosyl-5H-[1,3]dithiolo[4,5-c]pyrrol-2-one,[9] 2,5-bis[(*p*-tolyl)hydroxymethyl]thiophene,[10] 5,5'-bis[(*p*-tolyl)hydroxymethyl]-2,2'-bithiophene[10], *meso*-Tolyl-substituted dithiaporphyrin (S_2TTP)[11], and *meso*-Tolyl substituted tetrathiarubyrin (S_4TTR)[12], were synthesized using previously reported procedures.

Density Functional Theory (DFT) Calculations. Theoretical calculations were performed with the *Gaussian09* program suite using a supercomputer.[13] All calculations were carried out using the density functional theory (DFT) method with Becke's three-parameter hybrid exchange functionals and the Lee-Yang-Parr correlation functional (B3LYP) employing the 6-31G(d) basis set for all atoms.[14]

Synthesis of C_6S-TTF-pyrrole: 4,5-Bis(hexylthio)-1,3-dithiole-2-thione (1.89 g, 5.154 mmol) and 5-tosyl-5H-[1,3]dithiolo[4,5-c]pyrrol-2-one (0.7 g, 2.248 mmol) were suspended in triethylposphite (15.0 mL) and the reaction mixture was stirred at 140-145^{o}C in pre-heated oil bath for 5 h under nitrogen atmosphere. Then cooled to room temperature, the product mixture was kept in deep freeze for overnight and then filtered the cold solution. The obtained yellow solid was washed with hexane for several times to remove an impurity of symmetrical TTF compound. The compound can be used directly without any further purification. Yield: 1.05 g, ca. 74 % ^{1}H NMR (300 MHz, $CDCl_3$): δ 0.88 (t, 6H, CH_3), 1.25-1.33 (m, 8H, CH_2), 1.34-1.44 (m, 4H, CH_2), 1.56-1.66 (m, 4H, CH_2), 2.42 (s, 3H, $ArCH_3$), 2.80 (t, 4H, SCH_2), 6.93 (s, 2H, α-H), 7.30 (d, J = 8.0 Hz, 2H, Ar-H), 7.73 (d, J = 8.0 Hz, 2H, Ar-H) ppm.

A suspension of tosyl protected TTF pyrrole (0.4 g, 0.635 mmol) in anhydrous THF-MeOH (1:1 v/v, 20 mL) was degassed by N_2 for 15 min before addition of sodium methoxide (30% solution in MeOH, 2.35 mL) in one portion. The yellow reaction mixture was refluxed for 20 min. The reaction mixture was cooled to room temperature and concentrated to approximately 2 mL, and then ammonium chloride solution (5 mL) was added. The resulting yellow precipitate was extracted into dichloromethane, washed with brain solution and water and dried over Na_2SO_4. Purificaition by silica column chromatography using dichloromethane/hexane (1/2) as eluent gave yellow solid of **7**. Yield: 0.215 g, 71 %, ^{1}H NMR (300 MHz, $CDCl_3$): 0.89 (t, 6H, CH_3), 1.25-1.34 (m, 8H, CH_2), 1.36-1.45 (m, 4H, CH_2), 1.58-1.68 (m, 4H, CH_2), 2.82 (t, 4H, SCH_2), 6.60 (s, 2H, α-H), 8.1 (br s, 1H, NH) ppm.

General Synthetic procedure for TTF-annulated porphyrins

A dichloromethane solution (360 mL) of the corresponding thiophene (**8**) and bithiophene (**9**) diols (0.5 mmol), respectively, and TTF annulated pyrrole **7** (0.5 mmol) was purging with N_2 gas before adding acid catalyst, BF_3•Et_2O (0.25 mmol). The reaction mixture was stirred for 1 hour. DDQ (1.5 mmol) was then added to the mixture and stirred further for 30 min in air. Triethylamine (0.3 mL) was added to quench the reaction. The crude residues thus obtained were recrystallized in MeOH solvent by sonication and filtered. The desired porphyrin compound **1** was purifed over silica gel eluted with CH_2Cl_2, and rubyrin compound **2** was eluted chloroform:hexane (1:1) on basic alumina column chromatography. The samples for experiments were further purified by recrystallization in $CHCl_3$/MeOH solvents .

TTF-annulated dithiaporphyrin 1: Yield: 28%; ^{1}H NMR (300 MHz, $CDCl_3$): δ 0.90 (t, J = 7.0 Hz, 12H, CH_3), 1.26-1.32 (m, 16H, CH_2), 1.38-1.47 (m, 8H, CH_2), 1.59-1.69 (q, *J* = 7.4 Hz, 8H, CH_2), 2.76 (s, 12H, $ArCH_3$), 2.82 (t, *J* = 7.4 Hz, 8H, SCH_2), 7.66 (d, *J* = 7.8Hz, 8H, Ar-H), 7.94 (d, *J* = 7.8Hz, 8H, Ar-H), 9.48 (s, 4H, β-H); ^{13}C NMR (100 MHz, $CDCl_3$) δ 147.8, 147.3, 141.8, 139.2, 136.8, 135.8, 132.8, 132.5, 132.1, 129.5, 129.3, 127.8, 36.3, 31.3, 29.7, 28.2, 22.5, 21.7, 14.0 ppm. HRMS (FAB) *m/z* = 1520.2729 (found), 1520.2724 (Calcd. for $C_{80}H_{84}N_2S_{14}^+$), Error; +0.3 ppm. UV/Vis [in Toluene, λ_{max}/nm (log ε)]: 448 (5.54), 521 (4.62), 572 (3.66), 636 (3.63), 693(3.65).

TTF-annulated tetrathiarubyrin 2: Yield: 13%; ^{1}H NMR (400 MHz, $CDCl_3$): δ 0.91 (t, *J* = 7.0 Hz, 12H, CH_3), 1.28-1.35 (m, 16H, CH_2), 1.42-1.50 (m, 8H, CH_2), 1.65-1.84 (q, *J* = 7.4 Hz, 8H, CH_2), 2.88 (t, *J* = 7.4 Hz, 8H, SCH_2), 2.92 (s, 12H, $ArCH_3$), 7.85 (d, *J* = 7.6 Hz, 8H, Ar-H), 8.24 (d, *J* = 7.6Hz, 8H, Ar-H), 10.26 (d, *J* = 5.0 Hz, 8H, β-H), 11.49 (d, *J* = 5.0 Hz, 8H, β-H); ^{13}C NMR (100 MHz, $CDCl_3$) δ 144.0, 141.7, 141.2, 139.3, 138.4, 135.5, 133.2, 129.9, 129.3, 127.9, 124.8, 106.24, 36.4, 31.3, 29.8, 28.3, 22.5, 21.9, 14.0 ppm. HRMS (FAB) *m/z* = 1684.2478 (found), 1684.2479 (Calcd. for $C_{88}H_{88}N_2S_{16}^+$), Error; –0.1 ppm. UV/Vis [in Toluene, λ_{max}/nm (log ε)]: 545 (6.02), 670 (4.61), 731 (4.91), 846 (4.16).

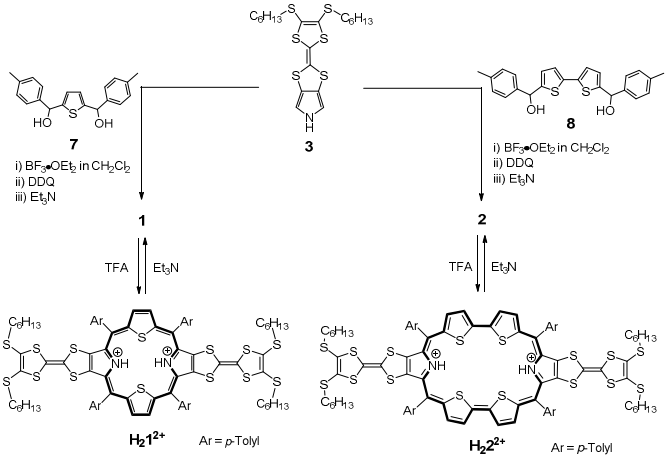

Scheme 1. Synthesis of TTF-annulated dithiaporphyrin **1** and -tetrathiarubyrin **2** and conversion to their protonated forms

Results and Discussion

Synthesis and characterization of 1 and 2. The TTF-annulated dithiaporphyrin **1**, and tetrathiarubyrin **2** were prepared by conventional one-pot condensation of TTF-annulated pyrrole (**7**) with the appropriate carbinol (i.e., 2,5-bis[(*p*-tolyl)hydroxymethyl]thiophene (**8**)[10] or 5,5'-bis[(*p*-tolyl)hydroxymethyl]-2,2'-bithiophene (**9**)[10] in the presence of boron trifluoride and followed by 2,3-dichloro-5,6-dicyano-*p*-benzoquinone (DDQ) oxidation. Macrocycles **1** and **2** were well characterized by spectroscopic means including NMR, Mass spectrometry and HPLC techniques (*cf.* ESI).

In the ^{1}H NMR spectra, the signal corresponding to β-thiophene-Hs appeared as a singlet at δ 9.48 ppm for **1** and as two doublets at 11.49 (*J* = 5.0 Hz) and 10.28 (*J* = 5.0 Hz) ppm for **2** are seen, which are indicative of typical aromatic character due to the diatropic ring current of the macrocycles (Fig. S2 and S5).[4a,11,12] In particular, it is concluded that a highly symmetric and the planar rectangle conformation of the core of **2** is thus present in solution as considering the characteristic NMR resonance patterns of the unsubstituted rubyrin (S_4TTR).[12] In order to gain the structural insights of the macrocycle, the density functional theory (DFT) calculations were carried out by using the B3LYP/6-31G(d) levels. Compared to the structures of the unfunctionalized derivatives, S_2TTP and S_4TTR, the relatively coplanar conformations for **1** and **2** were demonstrated with mean deviation values (defined by porphyrin core atoms) of 0.087 and 0.332 Å, respectively (Fig. S10). The nucleus-independent chemical shift (NICS) values at their central values of the mean cores (e.g., −15.2 ppm for **1** and −14.1 ppm for **2**) support the distinct aromaticity of **1** and **2**, which are well consistent with the NMR spectroscopic observations.

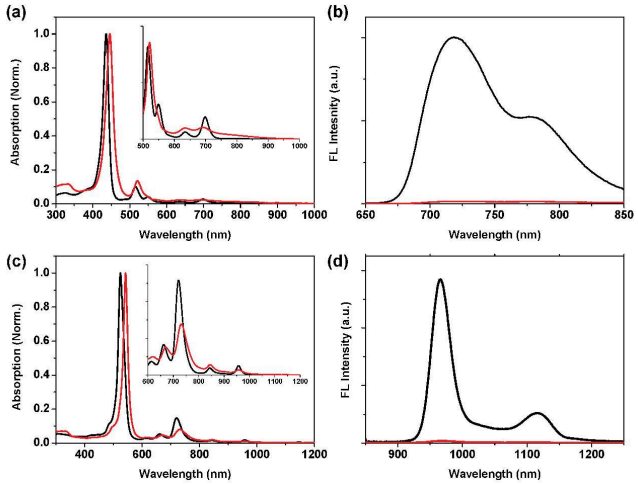

Fig 1. Comparative UV-vis-NIR absorption spectra of the porphyrins between (a) **1** (red) and S_2TTP (black), and the rubyrins; (c) **2** (red) and S_4TTR (black) recorded in CH_2Cl_2. Insets show the magnified region of Q-band, respectively. Emission

spectra of compounds (b) **1** (red) and S_2TTP (black) and (d) **2** (red) and S_4TTR (black) are given.

Optical properties and DFT calculations. These 18 π- and 26 π-electron compounds, **1** and **2** exhibited the typical optical features in the UV-vis-NIR absorption spectroscopy. The redshifted Soret band and broad Q-bands tailing to the 1000 nm in **1** were seen in CH_2Cl_2 in comparison with those of the non-annulated S_2TTP (Fig. 1a). This is due to the strong electronic coupling between the porphyrin core and the peripheral TTF fragments. Meanwhile, a broad lowest energy band could be attributed to the intramolecular charge transfer transition. The core modification present in **1** affords overall redshifts of absorption bands compared to the original pyrrole-based congeners (e.g., λ_{Soret} = 448 nm for **1** and λ_{Soret} = approximately 430 nm for **3** and **4**).[4] The photo-induced charge transfer event occurring in **1** was also confirmed by using fluorescence spectroscopy. The overall fluorescence of **1** is largely quenched compared to that of S_2TTP, which is may involve the electron transfer from TTF to the excited state of porphyrin core, leading to the rapid excited intramolecular charge transfer. (Fig. 1b). In the polar media such as THF, the emission intensities of **1** and **2** were further quenched, indicating possibly acceleration of the electron transfer rate (Fig. S11). As considered that N_4-porphyrin derivatives **3** and **4** has no detectable luminescence under the ambient condition, the core modifications of the porphyrin skeleton would effect on the inherent molecular orbital interactions between the donor TTF moiety and acceptor porphyrin core in **1**.[4]

In the π-expanded system of TTF-rubyrin **2**, due to the expansion of π-conjugation network, lower energy absorption bands are seen in the NIR region. The characteristic CT band originated from the TTF moieties to the rubyrin core unit was likewise appeared in the far NIR region (Fig. 1c). Consequently the fluorescence of **2** was quenched in comparison with S_4TTR as well (Fig. 1d).

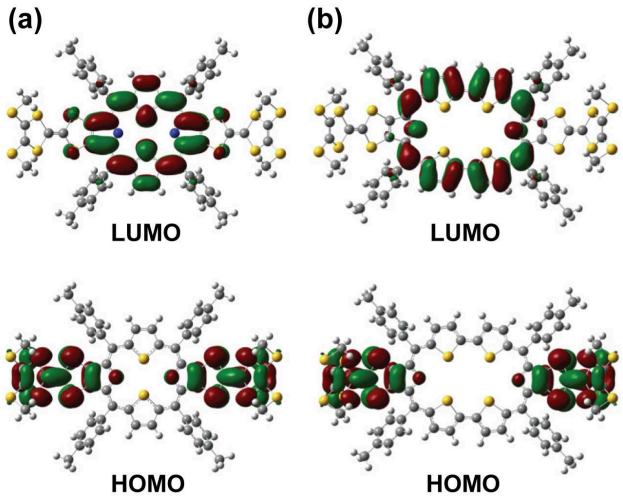

Fig. 2. Selected frontier molecular orbitals of (a) **1** and (b) **2** obtained by using B3LYP/6-31G(d) level calculations

The molecular orbital analysis (B3LYP/6-31G(d) levels) revealed that the electron densities of HOMO are localized on the TTF moieties whereas those of LUMOs are predominantly distributed on the whole macrocycle core for both cases, suggesting the presence of intramolecular charge transfer character (Fig. 2 and Fig. S12 and S13).[4] The latter MO energetic trend can be interpreted by the classical Goutermann's four orbital theory[16], and the broad CT band observed in the NIR region could thus be attributed to the HOMO-LUMO electronic transition. The time dependent (TD) DFT simulation of the electronic spectrum of **1** also supports the CT-based transition (oscillator strength, *f*; 0.0026) with the energy of 1.44 eV (Fig. S14a). These intramolecular interactions are found in those of TTF-annulated porphyrins **3** and **4**.[4] Accordingly, the energy trend of MO diagram of the π-expanded derivative **2** demonstrated the similar MO fashion; the TTF-based HOMO and HOMO-1 as well as the macrocycle-based MOs with degenerated HOMO-2 and HOMO-3 pair and the LUMO pair were found to be considered. The forbidden transition is identified with the CT nature (*f* = 0.0048, 1.31 eV) by TD-DFT calculation (Fig. S14b).

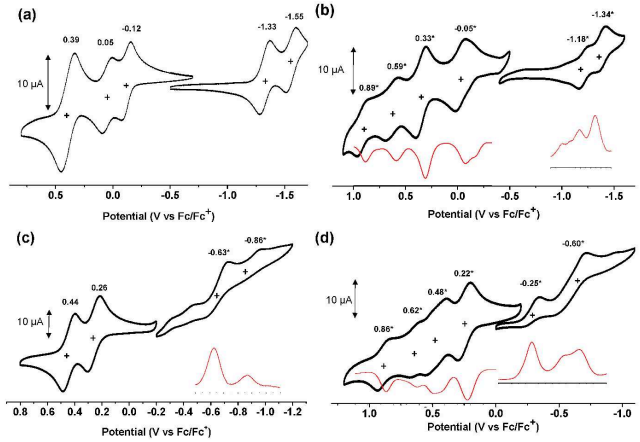

Fig. 3. Cyclic voltammograms of (a) **1**, (b) **2** (c) $\mathbf{H_2 1^{2+}}$ and (d) $\mathbf{H_2 2^{2+}}$ recoded in CH_2Cl_2 containing 0.1 M nBu_4NPF_6 as a supporting electrolyte. Insets show the differential pulse voltammograms (red line). [Compound] = 1 mM, Scan rate: 0.1 V/s, GC working electrode.

Redox properties. In an effort to determine the driving force for the electron transfer processes, the electrochemical potentials of **1** and **2** were measured by cyclic voltammetry (CV) and differential pulse voltammetry (DPV) technique in the CH_2Cl_2 containing 0.1 M *n*-tetrabutylammonium hexafluorophosphate ($TBAPF_6$) (Fig. 3). The compound **1** revealed two reversible one-electron oxidation waves located at –0.12 and 0.05 V (vs. ferrocene/ferrocenium couple) and a two-electron oxidation wave seen at 0.39 V in the anodic side. These peaks are corresponded to the TTF entities and the *trans*-symmetric orientation of the TTF moieties in **1** resulted in the separation of the first oxidation wave (for the process of TTF radical cation formation). This leads us to speculate the presence of electronic communication between the two TTF

units as considering the electrochemical behaviours of **3** and **4**. In the reduction side, two reversible waves corresponded to the radical anion and dianion of the porphyrin core are seen, which are significantly anodic shifted in comparison with the pyrrolic reference, **3** (E_{red} = –1.57 and –1.81 V vs. Fc/Fc^+), whereas the oxidation potentials were identical.[4] Accordingly, the narrower HOMO-LUMO electrochemical energy gap of 1.21 V in **1** reflected to the redshift of the optical bands. In the TTF-rubyrin system **2**, the TTF-based oxidation waves peaked at –0.05 and +0.33 V are both two-electron processes. This implies that the longer spatial separation of TTF arrangement causes less electronic interactions (diameter between inter TTF units is approx.17 Å for **2** vs. 14 Å for **1**). Further two oxidation waves originated from the radical cation and dication formations of the rubyrin core were observed at 0.59 and 0.89 V. The macrocyclic reductions at −1.18 and −1.34 V (vs. Fc/Fc^+) were determined on the basis of the comparative electrochemical study of S_4TTR (E_{red} = −0.86, −1.05 vs. SCE).[15] The further anodic shifts of the reduction potentials of **2** owing to the core π-expansion resulted in the narrow HOMO-LUMO gap of 1.13 V.

Photoinduced charge transfer. By using the electrochemical, optical and computational data, the relevant thermodynamic driving forces (ΔG_{CS}) for intramolecular charge separation were calculated using the *Rehm-Weller* equation.[17] By taking all the parameters into account, the estimated values of **1** and **2** are −0.48 eV and −0.31 eV, respectively. This result ensures that the electron transfer from the TTF units to the photo-excited porphyrin core is thermodynamically feasible reaction.

The supports for the formation of the proposed photoinduced charge separated species (i.e., $[(TTF)^{\bullet+}(P)^{\bullet-}(TTF)]$) of **1** and **2** were identified by EPR spectroscopy (Fig. S15). The EPR spectra of **1** and **2** recorded in CH_2Cl_2 exhibited a signal at g = 2.0058 and 2.0062 under Xe light irradiations, respectively, while the spectra taken under dark conditions were silent. The formation of TTF radical cation species in the chemical oxidations of **1** and **2** with tris(4-bromophenyl)aminium hexachloridoantimonate (known as Magic Blue) revealing EPR active signals at g tensor values of 2.0063 and 2.0065, respectively, are in consistent with those of the photoinduced electron transfer species.[18] The NIR absorption bands appearred in the oxidized species for **1** and **2** also support this conclusion (Fig. S16).

Protonation-induced charge transfer. Protonation of the pyrrolic nitrogen sites in the porphyrin ring could enhance the electron accepting ability due to the cationic electron-withdrawing effect in the core.[19] Therefore we thought that the driving force energies for intramolecular electron transfer of **1** and **2** could be fine-tuned upon protonation of the core-modified porphyrins. The electronic and redox properties of the dicationic species of **1** (i.e., $\mathbf{H_21}^{2+}$) and **2** ($\mathbf{H_22}^{2+}$) were significantly altered with those of the neutral species. The UV-vis-NIR absorption spectrum of $\mathbf{H_21}^{2+}$ exhibited a further redshifted Soret band along with an unprecedented broad CT band reaching >1700 nm (Fig. 4a). Likewise, the significantly broad Soret band appeared at 600 nm and featureless Q-like bands were observed in the rubyrin system **2** (Fig. 4b). The different choice of acids (e.g., methanesulfonic acid) also yielded the similar spectral features in the absorption spectroscopy (Fig. S17). The fluorescence emission are redshifted and furthermore quenched, in contrast to the fact that the unsubstituted dications ($H_2S_2TTP^{2+}$ and $H_2S_4TTR^{2+}$) exhibited the enhanced fluorescent emissions (Fig. S18). This imply the enhancement of the internal CT nature occuring in the protonated forms.

Upon addition of TFA, the ^{1}H NMR spectral signals of protonated species, $\mathbf{H_21}^{2+}$ and $\mathbf{H_22}^{2+}$ were not changed intially, however, further addition of TFA afforded broadening resonance peaks (Fig. S19-20). It is noteworhty that diprotonation of **1** or **2** with excess amount of TFA afforded the thermoexcited electron transfer products partially judging from active EPR signals at g = 2.0066 at room temperature (Fig.4c and 4d). [20] In this process, the formation of charge-separated species, i.e., $[(TTF)^{\bullet+}H_2P^{\bullet-}(TTF)]^{2+}\bullet 2TFA^-$ is thus assumed, since the cationic porphyrin core is a better electron transfer acceptor.[21] Upon neutralization with base (e.g., triethylamine) yielded the recovery of the oritinal spectra of **1** and **2**. The dual roles of triethylamine acting as a proton scavenger and a reducing agent may be accouted for the reversiblity.

In the electrochemical properties on the effect of protonation, both the oxidation and reduction potentials of $\mathbf{H_21}^{2+}$ and $\mathbf{H_22}^{2+}$ were anodically shifted (Fig. 3c and 3d). Particularly, the extent of the shifts of reduction waves was remarkable.[6] On this basis, protonation of the macrocyclic cores of **1** and **2** facilitates the intramolecular charge transfer as we expected. The resulting HOMO-LUMO gaps for $\mathbf{H_21}^{2+}$ and $\mathbf{H_22}^{2+}$ are estimated to be 0.89 and 0.47 V, which are well consistent with the observations of the NIR lower energy band (> 2000 nm) appeared in the absortpion spectra.

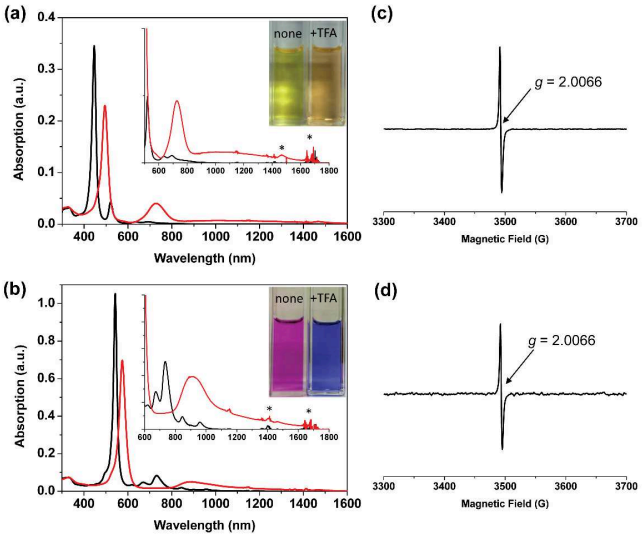

Fig 4. UV-Vis-NIR absorption spectral changes of (a) compound **1**(black) and $\mathbf{H_21}^{2+}$ (red) and (c) **2** (black) and $\mathbf{H_22}^{2+}$ (red) prepared in CH_2Cl_2 and EPR spectra of the protonated species (b) $\mathbf{H_21}^{2+}$ and (d) $\mathbf{H_22}^{2+}$ in the CH_2Cl_2/TFA mixture. Inset indicates the magnified NIR region and the photographs of the solution of neutral and deprotonated species for **1** and **2** taken under ambient light.

The DFT (B3LYP) calculations of the diprotonated species, $\mathbf{H_21}^{2+}$ and $\mathbf{H_22}^{2+}$ represent the deformation of the core structures and the extremely decreased energy gaps between HOMO and LUMO (i.e., ΔE = 1.13 V for $\mathbf{H_21}^{2+}$ and 0.66 V for $\mathbf{H_22}^{2+}$) resulted from the remarkable destabilization of the HOMOs (Figs. S21-22) in comparison with those of $H_2S_2TTP^{2+}$ and $H_2S_4TTR^{2+}$.[22] Such MO behaviour in the diagrams is not seen for the unsubstituted derivatives. As the matter of the fact, the TD-DFT simulations of $\mathbf{H_21}^{2+}$ and $\mathbf{H_22}^{2+}$ also support the presence of optically allowed electronic transitions in the NIR absoptions (Figs S23). The attachment of two protons therefore triggers the drastic perturbation in their electronic structures via effective expansion of the protonated π framework through appropriate orbital admixing at the appended sulfur atoms of TTF peripheries.

Conclusions

In summary, we have synthesised and characterized the first core-modified families of TTF-annulated porphyrin **1** and rubyrin **2**. In comparison with their photophysical properties of pyrrolic counterparts (i.e., **3** or **4**), the core modification in **1** was reflected in the difference of Gibbs driving force energies for electron transfer processes. The energetics of **1** were accounted for the facile reduction properties compared to the TTF-tetrapyrrolic porphyrin systems. Similarly, the negative driving force is seen in the expanded **2**. Furthermore, upon protonation of the macrocyclic cores, the energies for internal electron transfer could be enhanced due to the fact that protonation leads to the enhanced electron accepting ability of the macrocyclic core. Their HOMO-LUMO interactions were significantly changed as inferred by DFT calculations. Although the further studies on time-resolved laser spectroscopy is necessary to characterize the excited state dynamics of charge separation process, synthetic chemistry of these TTF-porphyrin ensembles would contribute the deep understanding of the photoinduced or thermal charge separation states. Furthermore, novel designs for organic materials tailored for electrochemically and optically controllable proton-electron coupled systems (e.g., artificial light harvesting antenna models) will be established.

Acknowledgements

We thank the Basic Science Research Program through the National Research Foundation of Korea (NRF) funded by the Ministry of Education, Science and Technology (2013R1A2A2A01004894) and Human Resource Training Project for Regional Innovation (No. 2013H1B8A2032078) for financial support. The work in Kyushu was supported by Grant-in-Aid (No. 26810024 to M.I. and 25248039 to H.F.) from Japan Society for the Promotion of Science (JSPS).

Notes and references

[a]*Department of Chemistry, Kangwon National University, ChunCheon 200-701, Korea*
[b]*Department of Chemistry and Biochemistry, Graduate School of Engineering and Education Center for Global Leaders in Molecular Systems for Devices, Kyushu University 744 Motooka, Nishi-ku, Fukuoka, 819-0395, Japan*
[c]*Department of Chemistry, BMS College of Engineering, Bull Temple Road, Bangalore 560019, India.*

† Electronic Supplementary Information (ESI) available: Supporting Figs and Schemes. See DOI: 10.1039/c000000x/

1. TTF Chemistry: Fundamentals and Applications of Tetrathiafulvalene; Yamada, J.; Sugimoto, T., Eds.; Springer: Berlin, 2004.
2. (a) P. Frère, P .J. Skabara, *Chem. Soc. Rev.,* 2005, **34**, 69-98; (b) D. Canevet, M. Sallè, G. Zhang, D. Zhang, D. Zhu, *Chem. Commun*., 2009, 2245-2269; (c) J. L. Segura, M. Martin, Angew. Chem. Int. Ed. Engl. 2001, **40**, 1372. (d) T. Sugawara, H. Komatsu K. Suzuki, *Chem. Soc. Rev.* 2011, **40**, 3105-3118.
3. (a) K. A. Nielsen, J. O. Jeppesen, E. Levillain, J. Becher, *Angew. Chem. Int. Ed.* 2003, **42**, 187–191; (b) K. A. Nielsen, W.-S. Cho, J. Lyskawa, E. Levillain, V. M. Lynch, J. L. Sessler, J. O. Jeppesen, *J. Am. Chem. Soc.* 2006, **128,** 2444–2451; (c) J. S. Park, E. Karnas, K. Ohkubo, P. Chen, K. M. Kadish, S. Fukuzumi, C. W. Bielawski, T. W. Hudnall, V. M. Lynch, J. L. Sessler, *Science* 2010, **329,** 1324–1327. (d) C. M. Davis, J. M. Lim, K. R. Larsen, D. S. Kim, Y. M. Sung, D. M. Lyons, V. M. Lynch, K. A. Nielsen, J. O. Jeppesen, D. Kim, J. S. Park J. L. Sessler, *J. Am. Chem. Soc*. 2014, **136**, 10410−10417.
4. (a) J. Becher, T. Brimert, J. O. Jeppesen, J. Z. Pedersen, R. Zubarev, T. Bjørnholm, N. Reitzel, T. R. Jensen, K. Kjaer, E. Levillain, *Angew. Chem. Int. Ed.,* 2001, **40**, 2497–2500; (b) H. Li, J. O. Jeppesen, E. Levillain, J. Becher, *Chem. Commun.* 2003, 846–847; (c) K. A. Nielsen, E. Levillain, V. M. Lynch, J. L. Sessler, J. O. Jeppesen, *Chem. Eur. J.* 2009, **15**, 506–516; (d) C. –G. Liu, W. Guan, P. Song, L. –K. Yan, Z. –M. Su, *Inorg. Chem*. 2009, **48**, 6548-6554. (e) Z. Wan, C. Jia, J. Zhang, X. Yao, Y. Shi, *Dyes Pigm.,* 2012, **93**, 1456–1462; (f) A. Jana, M. Ishida, K. Kwak, Y. M. Sung, D. S. Kim, V. M. Lynch, D. Lee, D. Kim, J. L. Sessler, *Chem. Eur. J.,* 2013, **19**, 338–349. (g) A. Jana, H. B. Gobeze, M. Ishida, T. Mori, K. Ariga, J. P. Hill, F. D'Souza, *Dalton Trans*., **2014**, *in press*.
5. (a) H. Jia, B. Schmid, S. –X. Liu, M. Jaggi, P. Monbaron, S. V. Bhosale, S. Rivadehi, S. J. Langford, L. Sanguinet, E. Levillain, M. E. El-Khouly, Y. Morita, S. Fukuzumi, S. Decurtins, *ChemPhysChem* 2012, **13**, 3370-3382; (b) A. Jana, M. Ishida, K. Cho, S. K. Ghosh, K. Kwak, K. Ohkubo, Y. M. Sung, C. M. Davis, V. M. Lynch, D. Lee, S. Fukuzumi, D. Kim, J. L. Sessler, *Chem. Commun.* 2013, **49**, 8937-8939.
6. L. Latos-Grazynski, In *Core Modified Hetero analogues of Porphyrins*; K. M. Kadish, K. M. Smith, R. Guilard, Eds.; Academic Press: New York, 2000; Vol. **2**. pp 361–416.
7. (a) Z. Zhang, W.-Y. Cha, N. J. Williams, E.L. Rush, M. Ishida, V. M. Lynch, D. Kim, J. L. Sessler, *J. Am. Chem. Soc*., 2014, **136**, 7591–7594; (b) M. Ishida, S.-J. Kim, C. Preihs, K. Ohkubo, J. M. Lim, B. S. Lee, J. S. Park, V. M. Lynch, V.r V. Roznyatovskiy, T. Sarma, P. K. Panda, C.-H. Lee, S. Fukuzumi, D. Kim, J. L Sessler, *Nature Chem*., 2013, **5**. 15-20.
8. Guo, K.; Yan, K.; Lu, X.; Qiu, Y.; Liu, Z.; Sun, J.; Yan, F.; Guo, W.; Yang, S. Org. Lett. 2012, 14, 2214-2217.

9. (a) Doi, I.; Miyazaki,E.; and Takimiya, K. Chem. Lett. 2008, 37, 1088. (b) Jeppesen, J. O.; Takimiya, K.; Jensen, F.; Brimert, T.; Nielsen, K.; Thorup, N.; Becher, J. J. Org. Chem. 2000, 65, 5794-5805. (c) Crivillers, N.; Oxtoby, N. S.; Mas-Torrent, M.; Veciana, J.; Rovira, C. Synthesis 2007, 11, 1621-1623.
10. Ulman, A.; Manassen, J. *J. Am. Chem. Soc*. 1975, **97**, 6540-6544.
11. Latos-Grazynski, L.; Lisowski, J.; Szterenberg, L.; Olmstead, M. M.; Balch, A. L. *J. Org. Chem*. 1991, **56**, 4043.
12. S. Rai, R. Manglampalli, *J. Porphyrins Phthalocyanines*, 2007, **11**, 784-794
13. Gaussian 09, Revision A.1, M. J. Frisch, G. W. Trucks, H. B. Schlegel, G. E. Scuseria, M. A. Robb, J. R. Cheeseman, G. Scalmani, V. Barone, B. Mennucci, G. A. Petersson, H. Nakatsuji, M. Caricato, X. Li, H. P. Hratchian, A. F. Izmaylov, J. Bloino, G. Zheng, J. L. Sonnenberg, M. Hada, M. Ehara, K. Toyota, R. Fukuda, J. Hasegawa, M. Ishida, T. Nakajima, Y. Honda, O. Kitao, H. Nakai, T. Vreven, J. A. Montgomery, Jr., J. E. Peralta, F. Ogliaro, M. Bearpark, J. J. Heyd, E. Brothers, K. N. Kudin, V. N. Staroverov, R. Kobayashi, J. Normand, K. Raghavachari, A. Rendell, J. C. Burant, S. S. Iyengar, J. Tomasi, M. Cossi, N. Rega, N. J. Millam, M. Klene, J. E. Knox, J. B. Cross, V. Bakken, C. Adamo, J. Jaramillo, R. Gomperts, R. E. Stratmann, O. Yazyev, A. J. Austin, R. Cammi, C. Pomelli, J. W. Ochterski, R. L. Martin, K. Morokuma, V. G. Zakrzewski, G. A. Voth, P. Salvador, J. J. Dannenberg, S. Dapprich, A. D. Daniels, Ö. Farkas, J. B. Foresman, J. V. Ortiz, J. Cioslowski and D. J. Fox Gaussian, Inc., Wallingford CT, 2009.
14. (a) A. D. Becke, *Phys. Rev. A*, 1988, **38**, 3098; (b) C. Lee, W. Yang and R. G. Parr, *Phys. Rev. B*, 1988, **37**, 785.
15. G. Santosh, M. Ravikanth, *Chem. Phys. Lett*., 2007, **448**, 248-252.
16. M. Goutermann, In the *Porphyrins* (ed.) D. Dolphin (New York: Academic Press) vol. 3, 1978.
17. N. Mataga, H. Miyasaka, in *Electron Transfer (Eds.: J. Jortner, M. Bixon)*, John Wiley and Sons, New York, 1999, 431-496.
18. The typical *g*-tensor values for the radical cation species of TTF-annulated pyrrole has been reported to be at approximately 2.008. See; ref 2c.
19. S. Fukuzumi, T. Honda, T. Kojima, *Coord. Chem. Rev*. 2012, **256**, 2488-2502.
20. The EPR spectra apparently favour to the formation of $[(TTF)^{\bullet+}H_2P(TTF)]^{3+}$, which was presumed that the *in situ* oxidation of the product by molecular dioxygen.
21. The covalently-linked TTF and tetracyanoquinodimethane (TCNQ) dyad has reported to show a thermoexcited electron transfer nature ($TTF^{\bullet+}$-σ-$TCNQ^{\bullet-}$) due to the extremely narrow HOMO-LUMO gap. See; D. F. Perepichka, M. R. Bryce, C. Pearson, M. C. Petty, E. J. L. McInnes, J. P. Zhao, *Angew. Chem. Int. Ed*., 2003, **42**, 4636-4639.
22. In order to explain the magnetic properties, we have examined the open shell electronic structures of $\mathbf{H_21}^{2+}$ and $\mathbf{H_22}^{2+}$ by using unrestricted B3LYP methods. The contribution of the open shell electronic species, such as dication biradicals were found to be thermodynamically unfovorable; the singlet and triplet energy gap were $\Delta E_{S\text{-}T}$ = 2.31 kcal/mol and 3.61 kcal/mol, respectively.

TOC

The effect of the core modification and protonation on the intramolecular charge transfer phenomenon was studied in the core-modified families of TTF-annulated porphyrinoids.